Charge-exchange and multi-scattering effects in (e,e′n) knockout

P. Demetriou, S. Boffi, C. Giusti and F. D. Pacati

Dipartimento di Fisica Nucleare e Teorica, Università di Pavia, and
Istituto Nazionale di Fisica Nucleare, Sezione di Pavia, Pavia, Italy

Abstract

Final-state interactions in (e,e′n) knockout reactions in the quasi-free region are studied by considering the multistep direct scattering of the ejectile nucleon. Primary and multiple particle emission are included within the same model and are found to become important with increasing excitation energy. Charge-exchange effects taken into account through the two-step (e,e′p) (p,n) and three-step (e,e′p) (p,N) (N,n) processes are also found to increase with energy. A comparison with the results obtained with an isospin-dependent optical potential at small excitation energies is presented.

1 Introduction

A large number of experiments on (e,e′p) reactions have been performed over the past years for a wide range of nuclei and kinematical regions. In the quasi-free (QF) region, the experimental cross sections are well described in the distorted-wave-impulse-approximation (DWIA), where the virtual photon interacts only with the emitted nucleon while the other nucleons are spectators and contribute to FSI only. Extensive comparisons between theoretical and

experimental cross sections, including the effects of FSI, have been able to provide insight on the s.p. properties of the nucleus [1].

On the other hand, additional and complementary information is, in principle, available from the (e,e′n) reaction. A comparison between (e,e′p) and (e,e′n) data taken in similar kinematics would allow us to study the different behaviour of protons and neutrons in nuclei. Experiments on the (e,e′n) reaction have not been made so far due to the difficulties in performing high-resolution neutron detection, particularly since theoretical predictions have shown the (e,e′n) cross sections to be significantly smaller than the (e,e′p) cross sections. Such an experimental comparison would however be of great interest for clarifying the reaction mechanisms, also in view of the fact that (γ, p) and (γ, n) cross sections have been observed to be of the same size [1]. From the theoretical point of view it is important to investigate the relevance of those processes which could play a different role in proton and neutron emission, and which might hamper the interpretation of data. In a series of papers [2, 3, 4] the effects of charge-exchange FSI was addressed. In [2] the (e,e′n) reaction was described as a direct mechanism accompanied by a two-step process, where a proton interacts with the virtual photon and then undergoes a (p,n) reaction. The charge-exchange process was treated as an isospin-flip in the final state interaction by an isospin dependent optical potential. The resulting cross sections showed a small effect arising from the charge-exchange contribution which decreased with the outgoing neutron energy. This was found to be in agreement with the results obtained within a self-consistent Hartree-Fock and continuum RPA model [3]. A different approach using a coupled-channels method in the lowest missing energy range [4] also predicted small contributions from charge-exchange processes.

In this paper we aim at investigating the (e,e′n) reaction in the QF region with particular interest in the effects of charge-exchange in FSI. The latter are described as a series of two-body NN interactions by means of the quantum-mechanical multistep direct theory (MSD) of [5]. Apart from direct neutron knockout, other processes contribute to the neutron emission spectra: the neutron after having absorbed the virtual photon undergoes several multistep scatterings before being emitted, and/or the virtual photon is absorbed by a proton which undergoes a charge-exchange reaction leading to neutron emission. The charge-exchange reaction can occur immediately after the photon absorption or after some re-scatterings.

At excitation energies above 50 MeV multi-nucleon emission can also occur through a multi-scattering mechanism. In this case the initially excited nucleon interacts with another nucleon exciting it to the continuum. Thus a secondary nucleon is emitted and may be detected giving rise to a different energy spectrum compared to the primary nucleon. The contribution of secondary nucleon emission to nucleon energy spectra has been investigated in nucleon-induced reactions by extending the theory of [5] and has been found to be important at high excitation energies [6]. We use the same method proposed by [6] to estimate the contribution of secondary neutrons to the (e,e′n) energy spectrum.

The theory of direct nucleon knockout reactions, primary MSD and multiple MSD reactions is presented in sect. 2. The results are given in sect. 3 and some conclusions are discussed in sect. 4.

2 Theory

2.1 Electroinduced direct nucleon knockout

The exclusive cross section for the (e,e′n) and (e,e′p) direct knockout reaction is obtained in the one-photon-exchange approximation. For an ejectile electron energy $E_{k'}$ and angle $\Omega_{k'}$ and ejectile neutron of energy E and angle Ω it can be written in terms of four structure functions [1]

$$\frac{\mathrm{d}^3\sigma}{\mathrm{d}\Omega_{k'}\mathrm{d}E_{k'}\mathrm{d}\Omega} = \frac{2\pi^2\alpha}{|\vec{q}|}\Gamma_{\mathrm{V}}\,K\{W_{\mathrm{T}}+\epsilon_{\mathrm{L}}\,W_{\mathrm{L}} + \sqrt{\epsilon_{\mathrm{L}}(1+\epsilon)}W_{\mathrm{TL}}\cos\phi+\epsilon\,W_{\mathrm{TT}}\cos 2\phi\}, \tag{1}$$

where Γ_{V} is the flux of virtual photons, ϕ the out-of-plane angle of the nucleon with respect to the electron scattering plane,

$$\epsilon = \left[1+2\frac{|\vec{q}|^2}{Q^2}\tan^2\tfrac{1}{2}\theta\right]^{-1}, \qquad \epsilon_{\mathrm{L}} = \frac{Q^2}{|\vec{q}|^2}\epsilon, \tag{2}$$

and $Q^2 = |\vec{q}|^2-\omega^2$ is the negative mass squared of the virtual photon defined in terms of the momentum $\vec{q}$ and energy ω transferred by the incident electron

through a scattering angle θ. Transitions to discrete final states are calculated with eq.(1) in DWIA and are extended to the continuum by including an energy distribution taken from [7] and described in [8].

2.2 Primary multistep emission

The details of the formalism have been presented in [8] so in the following we shall only give a brief account of the formulae used. The cross section for primary MSD emission is written as an incoherent sum of a direct neutron knockout (e,e′n) and multistep neutron emission cross sections

$$\frac{\mathrm{d}^4\sigma}{\mathrm{d}\Omega_{k'}\mathrm{d}E_{k'}\mathrm{d}\Omega\mathrm{d}E} = \frac{\mathrm{d}^4\sigma^{(1)}}{\mathrm{d}\Omega_{k'}\mathrm{d}E_{k'}\mathrm{d}\Omega\mathrm{d}E} + \sum_{n=2}^{\infty} \frac{\mathrm{d}^4\sigma^{(n)}}{\mathrm{d}\Omega_{k'}\mathrm{d}E_{k'}\mathrm{d}\Omega\mathrm{d}E}\,, \tag{3}$$

where the multistep (n-step) cross section is given by the convolution integral

$$\begin{aligned}\frac{\mathrm{d}^4\sigma^{(n)}}{\mathrm{d}\Omega_{k'}\mathrm{d}E_{k'}\mathrm{d}\Omega\mathrm{d}E} \quad = \quad & \left(\frac{m}{4\pi^2}\right)^{n-1} \int \mathrm{d}\Omega_{n-1} \int \mathrm{d}E_{n-1} E_{n-1} \ldots \\ & \times \int \mathrm{d}\Omega_1 \int \mathrm{d}E_1 E_1 \frac{\mathrm{d}^2\sigma^{(1)}}{\mathrm{d}\Omega dE}(\mathrm{n}, \mathrm{N}^{(n-1)}) \ldots \\ & \times \frac{\mathrm{d}^2\sigma^{(1)}}{\mathrm{d}\Omega_2\mathrm{d}E_2}(\mathrm{N}^{(2)}, \mathrm{N}^{(1)}) \frac{\mathrm{d}^4\sigma^{(1)}}{\mathrm{d}\Omega_{k'}\mathrm{d}E_{k'}\mathrm{d}\Omega_1 dE_1}(\mathrm{e}, \mathrm{e}'\mathrm{N}^{(1)})\,, \end{aligned} \tag{4}$$

over all intermediate energies $E_1,\ E_2 \ldots$ and angles $\Omega_1,\ \Omega_2 \ldots$ obeying energy and momentum conservation rules; m is the nucleon mass and N = n or p the particle excited in the intermediate one-step reactions (p = proton and n = neutron).

The one-step MSD cross section $\mathrm{d}^2\sigma^{(1)}/\mathrm{d}\Omega dE(\mathrm{N}^{(n)}, \mathrm{N}^{(n-1)})$ is calculated by extending DWBA to the continuum and is given by

$$\frac{\mathrm{d}^2\sigma^{(1)}}{\mathrm{d}\Omega\mathrm{d}E}(\mathrm{N}^{(n)}, \mathrm{N}^{(n-1)}) = \sum_J (2J+1)\rho_{1p1h,J}(U) \left\langle \frac{\mathrm{d}\sigma}{\mathrm{d}\Omega} \right\rangle_J^{\mathrm{DWBA}}\,, \tag{5}$$

where J is the orbital angular momentum transfer, $\langle \mathrm{d}\sigma/\mathrm{d}\Omega \rangle_J^{\mathrm{DWBA}}$ is the average of DWBA cross sections exciting $1p1h$ states consistent with energy,

angular momentum and parity conservation and $\rho_{1p1h,J}(U)$ is the density of such states with residual nucleus energy $U = E_{n-1} - E_n$. All possible inelastic or charge-exchange processes corresponding to $(\mathrm{N}^{(n)}, \mathrm{N}^{(n-1)})$ that can occur at the nth-step of FSI are estimated using eq.(5).

2.3 Multiple emission

Multiple pre-equilibrium emission in nucleon-induced reactions has been addressed by [6] using the theory of Feshbach *et al.* [5]. In their approach there exist two types of multiple emission: "type I", in which more than one excited particle is emitted immediately after a single intranuclear collision occurs; and "type II", where a particle is emitted after which a number of damping transitions occur, and then a second particle is emitted and so on. Their calculations showed that type II processes are relatively small compared to processes of type I and can therefore be omitted. In the following we apply the same formalism to multiple nucleon emission induced by electron scattering off the nucleus. We treat the multistep scatterings and multiple emission processes exactly as in nucleon-induced reactions assuming that the only difference in this case is the electromagnetic probe which appears in the cross sections for primary emission (eqs.3-5). We also restrict ourselves to processes in which up to two particles are emitted, though the formalism can be generalized to include more emissions.

According to [6], to determine the cross section for emission of a secondary particle at an energy E one starts with the cross section for producing particle-hole $(p-h)$ states at energy U after primary emission at stage n. The cross section at each n is given by eq.(4). Then one determines the probability that among such states there exists a nucleon with energy $E + E_{b.s.}$ (where $E_{b.s.}$ is the separation energy) which can escape with transmission-coefficient probability. A basic assumption here is that all possible $p-h$ configurations are equiprobable. The angle-integrated cross section is then given as the sum of contributions from each primary emission step n as follows

$$\frac{\mathrm{d}^3\sigma_{mul}^{(j)}}{\mathrm{d}\Omega_{k'}\mathrm{d}E_{k'}\mathrm{d}E} = \sum_n \frac{\mathrm{d}^3\sigma_{mul}^{(n,j)}}{\mathrm{d}\Omega_{k'}\mathrm{d}E_{k'}\mathrm{d}E}\,, \tag{6}$$

where

$$\frac{\mathrm{d}^3\sigma_{mul}^{(n,j)}}{\mathrm{d}\Omega_{k'}\mathrm{d}E_{k'}\mathrm{d}E} = \sum_{i=\mathrm{p,n}} \int_{U=E+E_{b.s.}}^{U_{max}} \frac{\mathrm{d}^3\sigma^{(n,i)}}{\mathrm{d}\Omega_{k'}\mathrm{d}E_{k'}\mathrm{d}U}$$
$$\times \left[\frac{1}{p}\frac{\omega(1p,0,E+E_{b.s.})\omega(p-1,h,U-E-E_{b.s.})}{\omega(p,h,U)}R_n^{i,j}\right] T_j(E)\,\mathrm{d}U, \quad (7)$$

where E is the emission energy, i labels the primary particle emitted (p = proton, n = neutron) and j the multiple particle emitted. The quantity in the square brackets is the probability of finding a particle j at an energy $E+E_{b.s.}$ inside a $p-h$ configuration of energy U, with $\omega(p,h,U)$ being the Fermi gas level density at excitation energy U. $R_n^{i,j}$ is the probability of finding a nucleon of type j in the $p-h$ configuration after primary emission of nucleon type i at step n and is calculated as prescribed by [9], $\mathrm{d}^3\sigma^{(n,i)}/\mathrm{d}\Omega_{k'}\mathrm{d}E_{k'}\mathrm{d}U$ is the differential cross section of $p-h$ states after primary emission of a nucleon type i at stage n. It is given as a function of the residual nucleus energy and is obtained by angle-integration of the cross sections of eq.(4). T_j is a Gamow penetrability factor and describes the probability that the continuum particle j escapes with an energy E.

The particles emitted through multiple and primary emission are given the same angular distribution through the following equation

$$\frac{\mathrm{d}^4\sigma_{mul}^{(n,j)}}{\mathrm{d}\Omega_{k'}\mathrm{d}E_{k'}\mathrm{d}\Omega\mathrm{d}E} = \frac{\mathrm{d}^3\sigma_{mul}^{(n,j)}}{\mathrm{d}\Omega_{k'}\mathrm{d}E_{k'}\mathrm{d}E}G(\Omega), \quad (8)$$

where the angular kernel $G(\Omega)$ is determined from eq.(4) as:

$$G(\Omega) = (\mathrm{d}^4\sigma^{(n,j)}/\mathrm{d}\Omega_{k'}\mathrm{d}E_{k'}\mathrm{d}\Omega\mathrm{d}E)/(\mathrm{d}^3\sigma^{(n,j)}/\mathrm{d}\Omega_{k'}\mathrm{d}E_{k'}\mathrm{d}E). \quad (9)$$

3 Results

The calculations of the (e,e′N) direct knockout cross sections and primary MSD cross sections were performed using the same input parameters as in [8]. The distorted waves were obtained from the optical potential of [10] and the b.s. wavefunctions from a Woods-Saxon potential with the geometrical parameters of [11]. The energy level densities involved in the primary MSD and

multiple emission cross sections were obtained from an equidistant Fermi-gas model with finite hole-depth restrictions [12] and an average single-particle density $g = A/13$ and the spin distribution was taken to be Gaussian with a spin cut-off parameter σ_n^2 of [13]. The multiple MSD cross-sections were calculated using computer subroutines developed by [14].

The method was applied to the (e,e′n) reaction on ^{40}Ca which is a suitable nucleus for the statistical assumptions of the MSD theory. Identical kinematic conditions as those in [8] were used, i.e, incident electron energy $E_k = 497$ MeV and electron scattering angle $\theta = 52.9°$. We fixed the scattered electron energy at $E_{k'} = 350$ MeV and worked at constant $(\vec{q}, \omega)$ by varying the neutron energy E accordingly.

In figure 1 we show the theoretical direct (e,e′n) knockout and multistep emission angular distributions at four excitation energies. The angle γ corresponds to the angle between the outgoing neutron $\vec{p}$ and momentum transfer $\vec{q}$. The multistep emission curves include contributions from all possible multistep scatterings of a n or p following photon absorption that end up in a neutron being emitted. For the three-step emission for example, we take into account the (e,e′n′) (n′,N) (N,n) and the (e,e′p) (p,N) (N,n) processes. At these excitation energies we compare only the direct knockout cross sections with the primary MSD emission cross sections.

The results show that the direct knock-out (e,e′n) process is dominant only at the lower excitation energies (lower missing energies) and even then only at forward angles (missing momentum $p_m \leq 200$ MeV/c). The multistep scattering cross sections increase with energy and scattering angles and at the higher excitation energies account for almost all the emission cross section. This is due to the large contributions from the two-step (e,e′p) (p,n) and three-step (e,e′p) (p,N) (N,n) processes which involve charge-exchange reactions. In fact, the contributions of these multistep processes are much larger than those from the (e,e′n′) (n′,n) and (e,e′n′) (n′,N) (N,n) processes. At the lowest missing energy the effect of charge-exchange contributions amounts to only ≈ 30 % of the total cross section, however it increases rapidly at large scattering angles and excitation energies.

It is worth comparing these results with those obtained using an isospin-dependent optical potential to account for charge-exchange contributions as reported in [2]. In figure 2 we present the angular distribution for the direct

knockout of a neutron from the $1s_{1/2}$ orbit in ^{40}Ca using the same kinematic conditions as in the case of figure 1. The residual nucleus is left at an excitation energy $U = 22$ MeV which roughly corresponds to the lowest excitation energy included in figure 1 so a comparison is possible. The cross sections with charge-exchange effects from an optical potential are identical to those obtained without charge-exchange and this can be clearly seen by plotting the difference between the two results (dotted line) in the same figure. The effect is of the order of $\approx 1 - 2\,\%$ in contrast with the $\approx 30\%$ effect given by multi-scattering contributions at the same excitation energy in figure 1. Therefore with the present approach of explicitly including multi-scattering effects in FSI, charge-exchange contributions are small at low missing energies confirming the dominance of the direct knockout mechanism in these energy regions, yet they are not as negligible as found in previous works.

In figures 3 and 4 we show the excitation energy spectra for neutron emission at two different sets of neutron scattering angles $\gamma = 0°$, $\phi = 0°$ and $\gamma = 30°$, $\phi = 0°$ respectively. Contributions from primary MSD and secondary MSD emission are included. At energies above the two-nucleon emission threshold a secondary neutron can be emitted along with a primary neutron or proton. Furthermore, primary neutron or proton emission result from either a (e,e′n) or (e,e′p) reaction so all processes such as (e,e′n′) (n′,xn), (e,e′p) (p,xn) including further re-scatterings are taken into account. At $\gamma = 0°$ and at low excitation energies direct neutron knockout is dominant in agreement with figure 1. However primary MSD emission is also important and becomes the dominant process with increasing energy and scattering angle as can be seen in figure 4. Charge-exchange processes which give the major contribution to primary MSD emission have already been included in the curves. Multiple particle emission also tends to increase with excitation energy and scattering angles as is seen by comparing figures 3 and 4. It seems that at larger scattering angles the strength is shifted from primary MSD to multiple MSD processes. The most important multiple emission contribution comes from two-step (e,e′p) (p,xn) which is comparable in magnitude with that of the primary three-and four-step MSD processes even at the lower excitation energies. Two-step secondary neutron emission is equivalent to a knockout mechanism in which a nucleon excited by a one-photon exchange mechanism strikes a bound neutron and both particles are emitted. In this respect it is quite similar to direct two-nucleon knockout which arises from

meson-exhange mechanisms (MEC) and short-range correlations (SRC) and has also been found to be important above the two-nucleon emission threshold for the ^{12}C(e,e′p) reaction [15].

4 Conclusions

We have treated FSI in the ^{40}Ca(e,e′n) reaction using the MSD theory of [5]. With this approach we are able to describe cross sections in the continuum thus our conclusions apply only to this region. We have shown that processes arising from an (e,e′p) reaction followed by charge-exchange MSD reactions (p,n) give the main contribution over the whole energy and angle range. Even at the lowest excitation energies and at the forward-scattering angles we find effects up to 30% which is larger than the estimates obtained with an isospin dependent optical potential. At excitation energies above the two-nucleon emission threshold secondary neutron emission has also been described within a multiple MSD model. The contributing cross sections are comparable in magnitude with those of three- and four-step primary neutron emission.

Charge-exchange processes in FSI have also been considered in two-nucleon knockout reactions. There the emission of a proton-proton pair is expected to be much lower than the emission of a proton-neutron pair. It has however been suggested that the former could be enhanced by contributions from two-step processes where a proton-neutron pair is first excited and then two protons are emitted via a charge-exchange process (e,e′pn) (n,p). So far such processes have been taken into account by means of an isospin-dependent optical potential [16] and have been found to be negligible. In view of the present results for primary and multiple MSD emission in one nucleon knockout reactions, it would be interesting to extend the MSD treatment of FSI to the (e,e′pp) and (e,e′pn) reaction to see to what extent charge-exchange in multistep processes will affect the relevant cross sections.

Acknowledgements

One of us (PD) would like to thank M. B. Chadwick for useful discussions and for providing the subroutines for the calculation of the multiple emission cross sections.

References

[1] S. Boffi, C. Giusti, F. D. Pacati and M. Radici, *Electromagnetic Response of Atomic Nuclei* (Clarendon Press, Oxford, 1996).

[2] C. Giusti and F. D. Pacati, Nucl. Phys. **A504** (1989) 685.

[3] J. Ryckebusch, K. Heyde, D. Van Neck and M. Waroquier, Nucl. Phys. **A503** (1989) 694.

[4] S. Jeschonnek, A. Szczurek, G. Co and S. Krewald, Nucl. Phys. **A570** (1994) 599.

[5] H. Feshbach, A. K. Kerman and S. Koonin, Ann. Phys. (NY) **125** (1980) 429.

[6] M. B. Chadwick, P. G. Young, D. C. George and Y. Watanabe, Phys. Rev. **C 50** (1994) 996.

[7] G. J. Kramer, PhD Thesis, University of Amsterdam (1990).

[8] P. Demetriou, S. Boffi, C. Giusti and F. D. Pacati, Nucl. Phys. **A** (in press).

[9] M. Blann and H. Vonach, Phys. Rev. **C 28** (1983) 1475.

[10] M. M. Giannini, G. Ricco and A. Zucchiatti, Ann. Phys. (NY) **124** (1980) 208.

[11] J. Mougey et al., Nucl. Phys. **A262** (1976) 461.

[12] F. C. Williams, Nucl. Phys. **A166** (1971) 231.

[13] C. Y. Fu, Nucl. Sci. Eng. **92** (1986) 440.

[14] M. B. Chadwick, private communication.

[15] C. Giusti and F. D. Pacati, Nucl. Phys. **A571** (1994) 694.

[16] C. Giusti and F. D. Pacati, Nucl. Phys. **A585** (1995) 618.

Figure captions

Fig. 1. Differential cross section for the ^{40}Ca(e,e$'$n) reaction as a function of the angle γ between the emitted neutron momentum and the momentum transfer at four different excitation energies U of the residual nucleus. Thin solid line for the direct (e,e$'$n) process; thin dashed, dot-dashed and dotted lines for the two-, three- and four-step processes arising from the (e,e$'$n) reaction. The corresponding thick lines are for the two-, three- and four-step processes respectively arising from the (e,e$'$p) reaction. The total result is given by the thick solid line.

Fig. 2. Differential cross section for the ^{40}Ca(e,e$'$n) reaction as a function of the angle γ between the emitted neutron momentum and the momentum transfer where the ejectile neutron is emitted from the 1s$_{1/2}$ orbit. The solid line corresponds to the direct (e,e$'$n) process without charge-exchange effects and the dotted line represents the difference between the cross sections with and without charge-exchange effects obtained from an isospin dependent optical potential.

Fig. 3. Excitation energy spectra for the ^{40}Ca(e,e$'$n) reaction at neutron scattering angles $\gamma = 0°$, $\phi = 0°$. The solid line is for the direct (e,e$'$n) knockout and thin dashed, dot-dashed and dotted lines for the two-, three- and four-step primary MSD processes respectively. The corresponding thick lines are for the two-, three- and four-step multiple MSD processes respectively.

Fig. 4. Same as Fig. 3 but for neutron scattering angles $\gamma = 30°$, $\phi = 0°$.

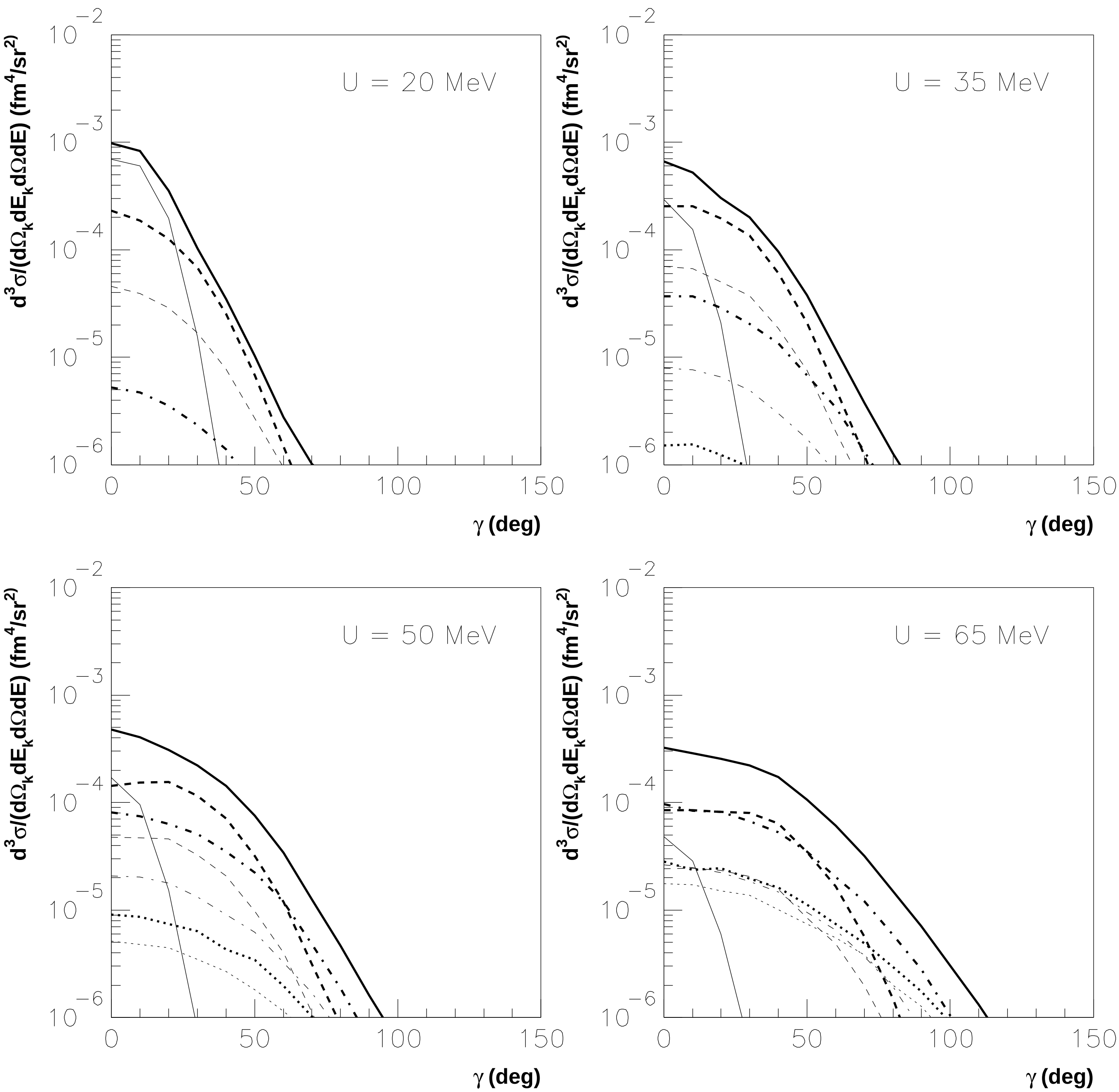
U = 20 MeV
U = 35 MeV
U = 50 MeV
U = 65 MeV
$d^3\sigma/(d\Omega_k dE_k d\Omega dE)$ (fm^4/sr^2)
γ (deg)
10^{-2}
10^{-3}
10^{-4}
10^{-5}
10^{-6}
0
50
100
150

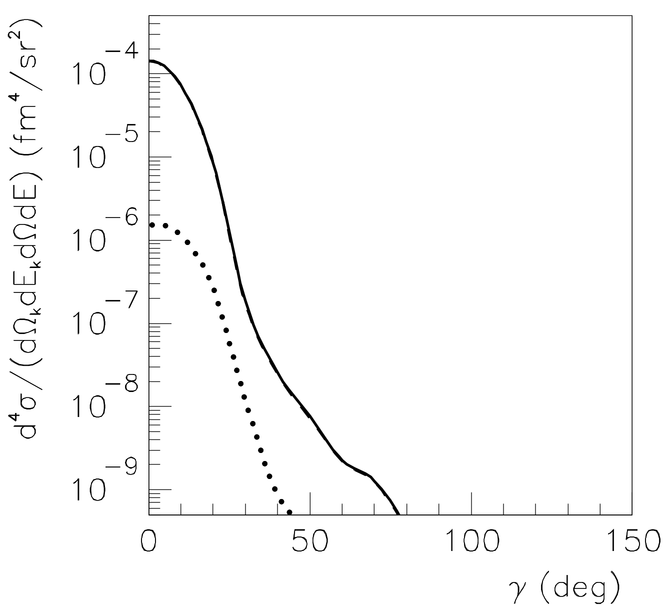

$d^4\sigma/(d\Omega_k dE_k d\Omega dE)$ (fm^4/sr^2)
10^{-4}
10^{-5}
10^{-6}
10^{-7}
10^{-8}
10^{-9}
0
50
100
150
γ (deg)

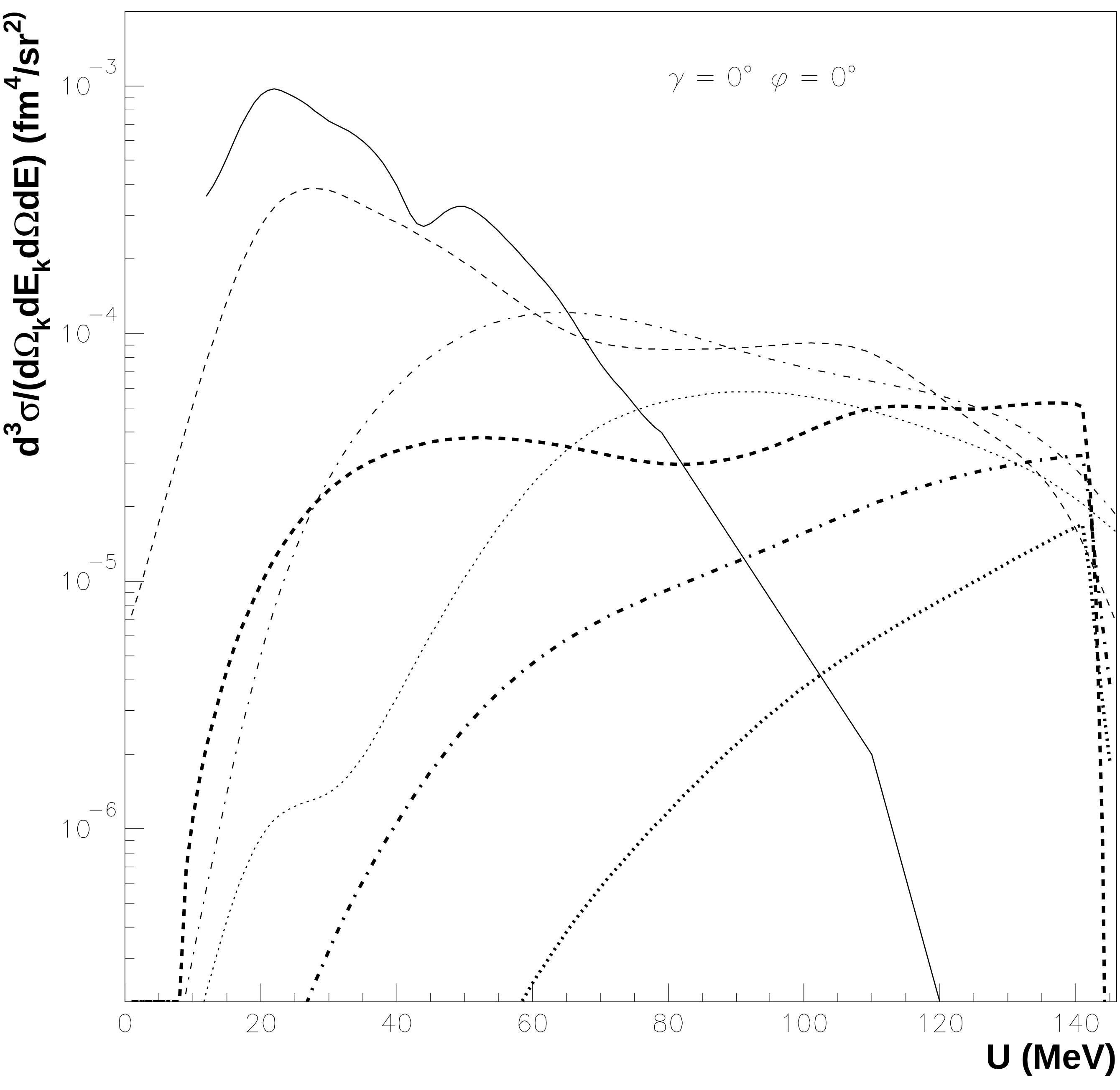

$\gamma = 0° \ \ \varphi = 0°$
$d^3\sigma/(d\Omega_k dE_k d\Omega dE)$ (fm^4/sr^2)
10^{-3}
10^{-4}
10^{-5}
10^{-6}
0
20
40
60
80
100
120
140
U (MeV)

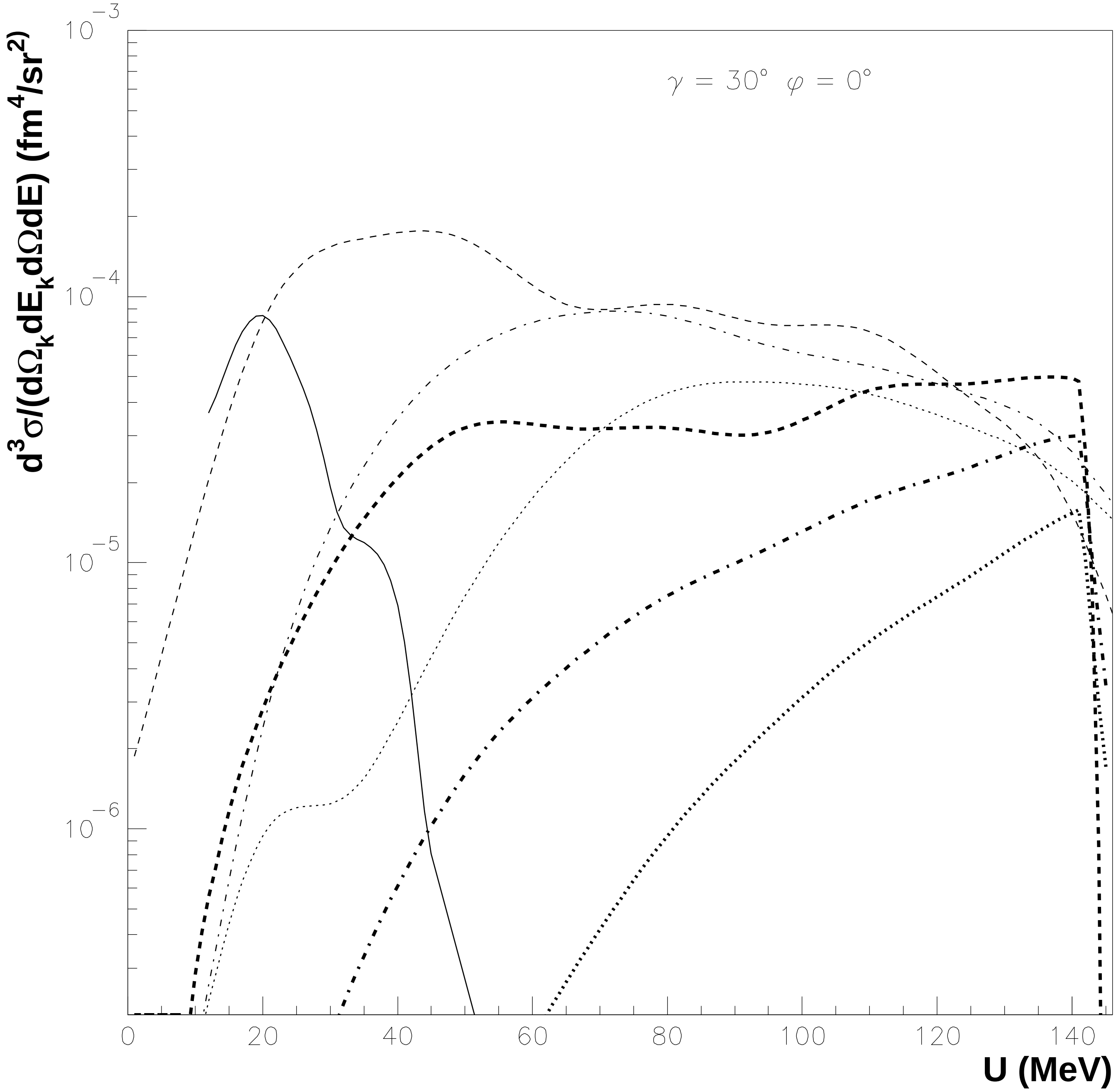
10^{-3}
10^{-4}
10^{-5}
10^{-6}
$\gamma = 30° \;\; \varphi = 0°$
$d^3\sigma/(d\Omega_k dE_k d\Omega dE)$ (fm^4/sr^2)
0
20
40
60
80
100
120
140
U (MeV)